Where to Dip?
Search Pattern for an Antisubmarine Helicopter Using a Dipping Sensor

Roey Ben Yoash, Michael P. Atkinson and Moshe Kress

Operations Research Department,
Naval Postgraduate School
Monterey, CA 93943

Abstract

Anti-submarine warfare (ASW) had been an important topic for military operation research (MilOR) modelers and analysts during World War II and the Cold War. It became however somewhat out of vogue with the collapse of the Soviet Union and the subsequent reduction of the threat of submarine-related conflicts. In recent years, threats of such engagement have increased, in particular in the South China Sea. The re-emerging interest in this type of warfare, combined with new technologies and resulting tactics, pose a renewed challenge for MilOR researchers. We study effective ways to operate a helicopter, equipped with dipping sonar – a *dipper* – in ASW missions. In particular, we examine the dipping pattern and frequency. A high rate of dipping is desirable as search effectiveness degrades in time as the search area expands. However, dipping too frequently results in overlap with previous dips, which may be wasteful. For a cookie-cutter sensor and a known constant submarine velocity, we prove that disjoint dips are optimal and generate the corresponding optimal dipping pattern. We analyze the effect of factors, such as helicopter speed, submarine speed, sensor detection radius, and travel time to the point of detection, on the optimal dipping pattern. We show that temporal parameters – submarine velocity and helicopter arrival time to the datum – are most critical. We also show that the no-overlap result is not always true; when the submarine's velocity is only known with probability, the optimal dipping frequency may include overlaps.

Military OR application area: Regional Sea Control

OR methodology: Probabilistic Operations Research; Decision in the presence of uncertainty

1. INTRODUCTION

Submarines pose a major threat to naval ships and therefore submarines become prime targets during naval operations. However, detecting and engaging these targets is challenging due to their stealth and high endurance. A common practice in modern anti-submarine warfare (ASW) is to send out helicopters equipped with dipping sonar, which allows the helicopter crew to listen for underwater signals while hovering at an altitude of 50 to 300 feet above sea level (Global Security, 2016). The helicopter uses a cable to lower the sensor to the desired depth, which can range from the just below the surface of the sea to 2,500 ft (Global Security, 2016). The dipping sonar is primarily an active sensor, and hence the sonar generates sound signals once lowered into position. Signal processing algorithms process the echoes that return to the sensor to locate enemy submarines (Global Security, 2016). In many situations, such helicopters are dispatched to search and hunt a submarine following a cue received from some exogenous surveillance source such as fixed-wing aircraft or towed arrays from surface ships. This source provides the location (known as the *datum*) of the suspected target and the time of detection. Given this datum, the question is what would be the optimal dipping pattern for the search helicopter. The shape and size of this pattern can indicate if it would be worthwhile to dispatch the helicopter. We examine a more specific question in this paper: given the current dipping location, when and where should the next dip occur? On one hand, the dipping frequency should be high as search effectiveness degrades in time as the submarine moves and the search area expands. On the other hand, dipping too frequently may result in overlap with previous dips, which may lower search efficiency.

The (mathematical) problem of search and detection has been studied for the past 70 years. The ground-breaking work of Koopman (Koopman, 1946) laid the foundation for this area of research. Other seminal works in general search theory are (Stone, 1975), (Haley and Stone, 1980), and (Washburn, 2002). Search models specific to ASW operations appear in (Shephard, et al., 1988), where a helicopter, equipped with sonar buoys and torpedoes, is out to hunt a submarine. Their model assumes a uniform deployment of the sonar buoys in the containment circle and computes the optimal payload of buoys and torpedoes.

Several papers study dipping sonar tactics. Baston and Bostock (1989) examine where a helicopter should drop a finite number of cookie-cutter bombs to destroy a mobile submarine. The two entities move on a one-dimensional line and this limits the spatial impact of the increasing search area, which is crucial for our analysis of the tradeoff between searching frequently vs. limiting search overlap. Washburn and Hohzaki (2001) and Soto (2000) consider mechanical limitations on a submarine's velocity. They transform the discrete dips into a continuous search rate and examine the problem from a random search perspective. Thus, there is no analysis of when and where to discretely dip next.

Danskin (1968) has a very similar setup to our problem with a cookie-cutter dipping sensor. He postulates that a discrete dipping spiral pattern may be particularly effective (we show under certain assumptions, it is optimal). However, Danskin does not calculate the specific time and location of individual dips. He assumes that dips will be disjoint, which is the primary focus of our analysis. In this paper, we show that, using a similar framework to Danskin's, disjoint dips are not necessarily optimal. Thomas and Washburn (1991) and Chuan (1988) also have a similar framework to our model. These papers (as well as Danksin (1968)) consider the decreasing effectiveness of dips over time as the search area increases. Thomas and Washburn (1991) formulate a complex dynamic program to generate a search plan. They do account for the negative impact of traveling too far for the next dip, but they do not explicitly consider the negative impact of overlap as the target can move to any cell in the region between dips. Chuan (1988) does allow for overlap in practice due to operational inefficiencies, but assumes that in theory the dips should be disjoint.

Washburn (2002) examines a cookie-cutter dipping problem, which he refers to as "Sprint and Drift", in Chapter 1.7. This is the only example we found that suggests there may be benefits from overlapping dips. However, the model in Washburn (2002) is one-dimensional, and there is no formal analysis for determining an optimal dipping policy. Washburn (2002) also suggests situations other than ASW dipping sonar search where a discrete glimpsing cookie-cutter approach, such as our model, might apply. A sensor aboard a mobile asset may only be able to operate effectively when the asset is stationary due to noise or vibrations. For example, in ecology predators periodically stop to better

localize their prey. In other scenarios, the searcher may move passively and activate the sensor only at discrete times and locations to mitigate counter-detection. While we focus on ASW dipping sonar in this paper, there are other applications where our models and results could be useful.

Our main contribution is in examining the tradeoff between dipping frequency and search overlaps. Most work takes for granted that dips should be disjoint. While we find that to be the case under some assumptions, disjoint dipping is not necessarily optimal under other assumptions. In this paper, we primarily focus on a deterministic submarine velocity. The main result is a provable optimal dipping pattern that dictates how the search helicopter should dynamically deploy its dipping sensor. The key characteristic of the optimal dipping pattern is that the next dip location is the closest valid dipping point to the current location that produces a disjoint dip. Additional insights relate to the effect of operational and physical parameters on the shape and size of the resulting search spiral. We also consider a random submarine velocity and show that the optimal dipping strategy may incorporate overlaps.

The rest of the paper is organized as follows. In the next section, we describe the operational setting, which is followed with the statement of the main result for a deterministic submarine velocity. We discuss the case of a non-deterministic distributed submarine velocity in the fourth section. The fifth section presents sensitivity analysis regarding some key operational and physical parameters for the deterministic case. In the sixth section, we assume some partial knowledge about the bearing of the hunted submarine and show how this knowledge affects the dipping pattern. Concluding remarks appear in the seventh section.

2. OPERATIONAL SETTING

A naval task force is equipped with an antisubmarine warfare helicopter whose role is to hunt and kill enemy submarines. The helicopter is dispatched upon receipt of information about the location of a potential submarine target. The source of such information is typically a long-range anti-sub patrol unit continuously surveying the operational area of the task force (e.g., P-8 anti-sub aircraft or a surface ship equipped with a sonar device or

even a satellite). Launching a helicopter for an ASW mission is costly both economically and operationally. In particular, the helicopter may have other competing missions. Arguably, the decision to launch the ASW helicopter should depend on the probability of mission success. This probability is affected by the distance from the launching site to the datum, the helicopter velocity and endurance, and the submarine velocity. These factors are manifested in the shape and size of the search spiral (see next section). Throughout most of this paper, we assume that the searcher knows the sub's velocity, and thus its distance from the datum, but not its bearing.

The helicopter is equipped with dipping sonar (henceforth referred to as a *dipper*), which is "a sonar transducer that is lowered into the water from a hovering antisubmarine warfare helicopter and recovered after the search is complete" (FreeDictionary, 2016). Depth matters for our analysis in that it affects how long it takes to deploy the dipper and reel it back. However, we take the dipping time to be a fixed constant, and thus for this paper we assume that the dipper has a two-dimensional circular cookie-cutter detection function. That is, the detection range is arbitrarily deep and we ignore possible evasive actions by the submarine going deeper or shallower. We also assume a perfect sensor: if the submarine is present within the dipper's circular footprint – the *detection circle* – the dipper will detect the submarine with certainty. Otherwise, the submarine remains undetected.

A perfect cookie-cutter sensor is a significant simplification. In reality the dynamics of sonar detection are quite complicated and depend upon the acoustic properties of the environment, which impact the transmission loss between the target and sensor (Lee and Kim, 2012). However, cookie-cutter sensors are commonly used in many maritime search and detection applications to generate insight. Random search, the cornerstone model for many search analyses, is based on a cookie-cutter sensor (see Chapter 2 of Washburn (2002)) and often provides similar results to more complicated and realistic detection dynamics (Lee and Kim, 2012). Furthermore, many ASW models use cookie-cutter sensors, including Danskin (1968), Shephard, et al., (1988), Baston and Bostock (1989), and Washburn (2002). Our goal is to provide a baseline modelling framework and generate initial results and insight. Future work can build upon our approach with more realistic detection functions.

3. DIPPING PATTERN FOR CONSTANT AND KNOWN SUBMARINE VELOCITY

While the velocity of the sub is assumed to be constant and known to the searcher, its bearing is unknown and assumed to be uniformly distributed on [0, 360^o]. This assumption is relaxed later in the paper. Thus, the location of uncertainty (LoU) – the possible locations in which the submarine may be present – is a circumference of a circle with a radius that is determined by the velocities of the sub and the helicopter, and the distance the helicopter has to travel to the datum.

A *dipping pattern* is a series of consecutive dipping points for the dipper. A dipping pattern is optimal if, for a given number of dipping points, it maximizes the probability of detection, or, for an infinite number of available dipping points it minimizes the expected time of detection. Because the sub velocity is assumed to be known, the searching helicopter would know exactly the submarine's location, had the searcher known the sub's heading. Thus, at any given time, the circumference of the circle around the datum on which the sub is located – the *location circle* – is uniquely determined. The *coverage* of a dip is the arc on the circumference of the location circle that is covered by a dip, which is equal to the angle α, rooted at the datum, between the two tangents to the detection circle (See Figure 1).

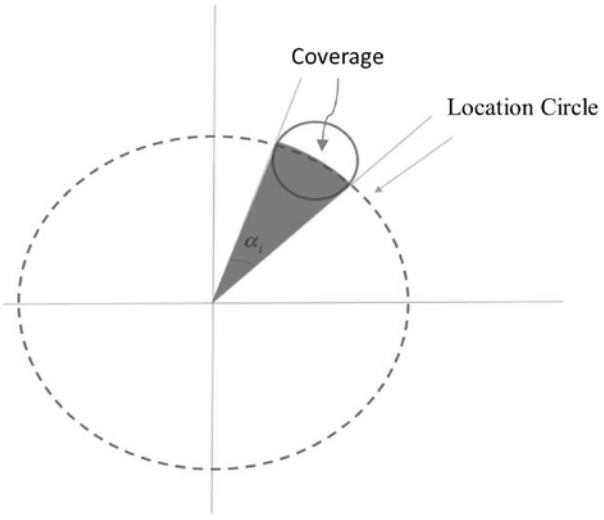

Figure 1: Location Circle and Coverage

Continuous search patterns over an expanding circle are well known to be a spiral with a shape dictated by the velocity of the sub (Washburn, 1980; 2002). As our search is discrete, we must determine where on the spiral to next dip. There are essentially three generic dipping patterns: *overlapping, tangential* and *excessively disjoint* (see Figure 2). Following a dip, the helicopter can travel a short distance and dip again (Figure 2a), in which case the coverage of the second dip is relatively large, but part of it overlaps with the coverage of the first dip.

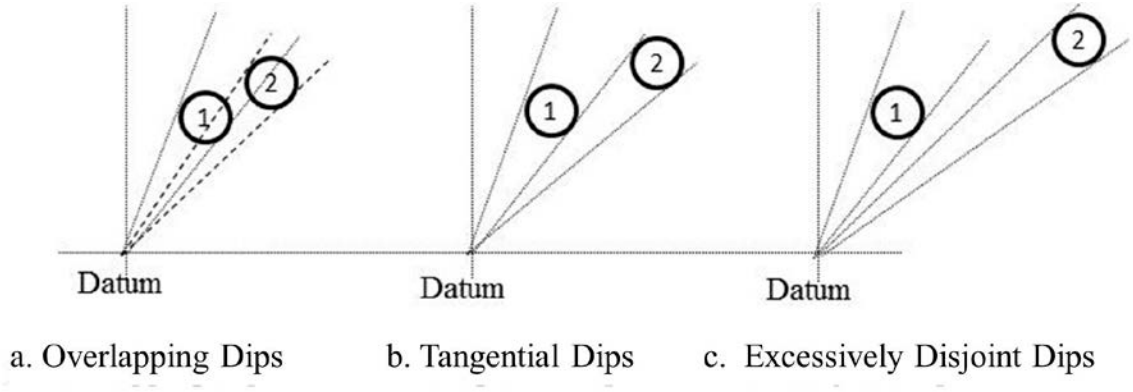

Figure 2: Dipping Patterns

If the helicopter travels farther away the coverage shrinks but the overlap disappears (Figure 2b). The tangential dip is the closest disjoint dip. If the helicopter travels even farther, the coverage is even smaller and there are some gaps in the area searched (Figure 2c). While, evidently, excessively disjoint dips are suboptimal, it is not obvious which of the two cases – overlapping dips or tangential dips – is better. Specifically, while dip 2 in Figure 2a has a larger coverage than dip 2 in Figure 2b, it is not clear if the *effective coverage* of dip 2 in Figure 2a, i.e., the angle between the right tangent of dip 2 and the right tangent of dip 1 in Figure 2a, is larger or smaller than the coverage of dip 2 in Figure 2b. We prove that the latter is true; tangential dipping is optimal.

Let *U* and *V* denote the velocities of the submarine and helicopter, respectively. The dipper detection range is *R* and the time duration of a dip is τ_D. Let (0,0) denote the location of the datum, $P_i = (X_i, Y_i)$ be the location of the *i*-th dipping point, and T_i is the time, measured from the moment the external surveillance source delivered the datum,

the *i*-th dip starts. In particular, T_1 is the time the helicopter arrives to the first dipping point.

Theorem 1: For a given number of dips, tangential dips maximize the probability of detection.

The proof of the theorem appears in Appendix A. An optimal dipping pattern appears in Figure 3. To derive the actual expressions for the *i*-th dipping point, P_i, and the start time of *i*-th dip, T_i, requires additional notation and solving simultaneous non-linear equations. Consequently, we defer presentation of these expressions to Appendix A.

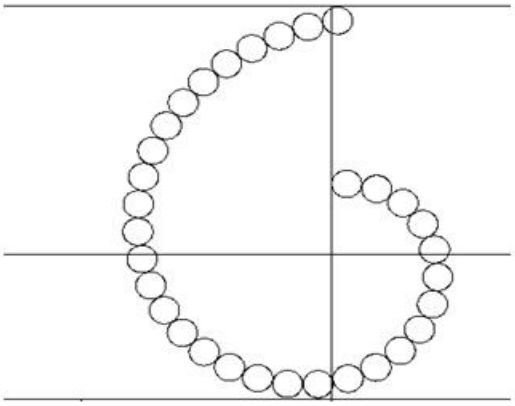

Figure 3: Optimal Dipping Pattern

We conclude this section by considering an imperfect cookie-cutter dipper. If the target lies within the footprint of the dipper, a detection only occurs with probability $0 < q < 1$. In this scenario, overlap has an additional benefit as it provides an opportunity to detect a previous false-negative. We assume the dip signals are independent across dips. The next theorem states that a tangential dipping policy is no longer necessarily optimal when the dipper is imperfect.

Theorem 2: When the dipper is an imperfect cookie-cutter sensor with detection probability $0 < q < 1$ within the sensor footprint, the optimal dipping frequency may include overlaps.

We prove Theorem 2 via a counterexample in Appendix B. In some cases it may be beneficial for one dip to completely overlap the previous dip. An overlap strategy is particularly effective when the time to reach the disjoint dipping location is relatively long. This occurs when the searcher is relatively slow (small V/U ratio) and the dip duration τ_D is short. A smaller value of the detection probability q also increases the importance of overlap. For realistic parameter values (e.g., large V/U ratio), the disjoint dipping strategy is usually close to optimal for the imperfect sensor case.

4. RANDOM SUBMARINE VELOCITY

Similarly to the framework described in Danskin (1968), suppose that immediately after the surveillance asset detects the submarine at the datum, the submarine's velocity and heading are randomly initialized, and the submarine maintains these two values throughout the search.

If the submarine's velocity is a random variable that takes on only a finite number of values, the analysis in Section 3 generalizes in a natural way with multiple spirals: one corresponding to each velocity. If there are multiple searchers, then each searcher dips on one spiral. If there is only one searcher, then we must determine the order the searcher should process the different velocity-spirals. For more details see (Ben Yoash, 2016).

In a more realistic case, the submarine's velocity is a continuous random variable. We assume a uniform bivariate distribution for the velocity and heading over the "speed-circle" (see Danskin (1968)), where the heading varies over $[0, 360^o]$ and the velocity varies over $[0, U_{max}]$. This implies that at time t the location of the submarine is uniformly distributed within a *containment circle* of radius $\rho(t) = U_{max} t$.

We next examine a similar tradeoff between timeliness and dipping overlaps as in the deterministic velocity case discussed in Section 3. For simplicity, we ignore here the dipping time τ_D. Given the dipper has a cookie-cutter detection function with radius *R*, and assuming the dip footprint is entirely within the containment circle, the probability the first dip detects the target is $\frac{R^2}{\rho^2(T_1)}$. If the second dip occurs at time $T_2 = T_1 + \Delta t$, then the contribution to the overall detection probability from the second dip is $\frac{\pi R^2 - \text{overlap}(\Delta t)}{\pi\rho^2(T_1 + \Delta t)}$, where $\text{overlap}(\Delta t)$ is the area of overlap between two circles: the second dip footprint and the area cleared by the first dip. For $\Delta t = 0$, there is complete overlap between the first two dips $(\text{overlap}(0) = \pi R^2)$, which results in a worthless search effort. For a large enough Δt, eventually there is no overlap $(\text{overlap}(\Delta t) = 0$, for large $\Delta t)$. The exact expression for $\text{overlap}(\Delta t)$ is somewhat complicated and appears in Appendix C. In general, $\text{overlap}(\Delta t)$ will decrease with Δt, and thus both the numerator and denominator increase in Δt. In Section 3 we showed, for the deterministic velocity case, that at optimality the next dip satisfies $\text{overlap}(\Delta t) = 0$: tangential dips are optimal. This is quite an intuitive result and it is taken for granted in other works (e.g., Chuan (1988), Danksin (1968)). The following theorem states that this result is not necessarily optimal when the submarine velocity is not deterministic.

Theorem 3: When the submarine heading and velocity have a bivariate uniform distribution over the speed circle of radius U_{max}, the optimal dipping frequency may include overlaps.

The details of the examples demonstrating this property require tedious calculations involving the area of the intersection of circles. We defer these examples to Appendix C. The optimal search pattern should include overlap when the helicopter arrives to the datum very soon after detection. The initial dip produces a relatively large detection probability. Because the detection probability from future dips decreases quickly (

$\propto (time)^{-2}$), the searcher benefits from taking the next dip soon after, even though the second dip partially overlaps with the first dip. The amount of overlap increases with a slow searcher as it takes longer to move to a location that produces a disjoint dip.

For most current ASW dipping scenarios, the helicopter will be much faster than the submarine, so a disjoint dipping strategy should be near optimal for most realistic parameters. To determine the specific times and locations for the optimal dipping pattern in the bivariate uniform scenario is a challenging problem that requires much more complicated machinery than we utilize in this paper. For an example of how one could proceed, see the dynamic programming approach in Thomas and Washburn (1991). For the remainder of the paper we return to the deterministic velocity scenario.

5. SENSITIVITY TO OPERATIONAL AND PHYSICAL PARAMETERS

Next we analyse the effect of operational and physical parameters on the shape of the optimal dipping pattern for deterministic submarine velocity. We start off with a base case that reflects typical values of the various parameters. Specifically, helicopter speed V = 100 knots, submarine speed U = 8 knots, time of arrival to first dipping point T_1 = 2 hrs, detection range R = 2 nm and dipping time τ_D = 5 min.

Helicopter's Speed (V)

The helicopter chases the submarine and therefore the faster the helicopter operates the smaller would be the area of uncertainty and therefore also the dipping spiral, as shown in Figure 4. While a velocity of V = 200 nm is obviously unrealistic for a helicopter, we observe that speed has decreasing marginal effect; the decrease in the spiral radius as a result of velocity increase from 50 knots to 100 knots is larger than the effect when the speed increases from 100 knots to 200 knots.

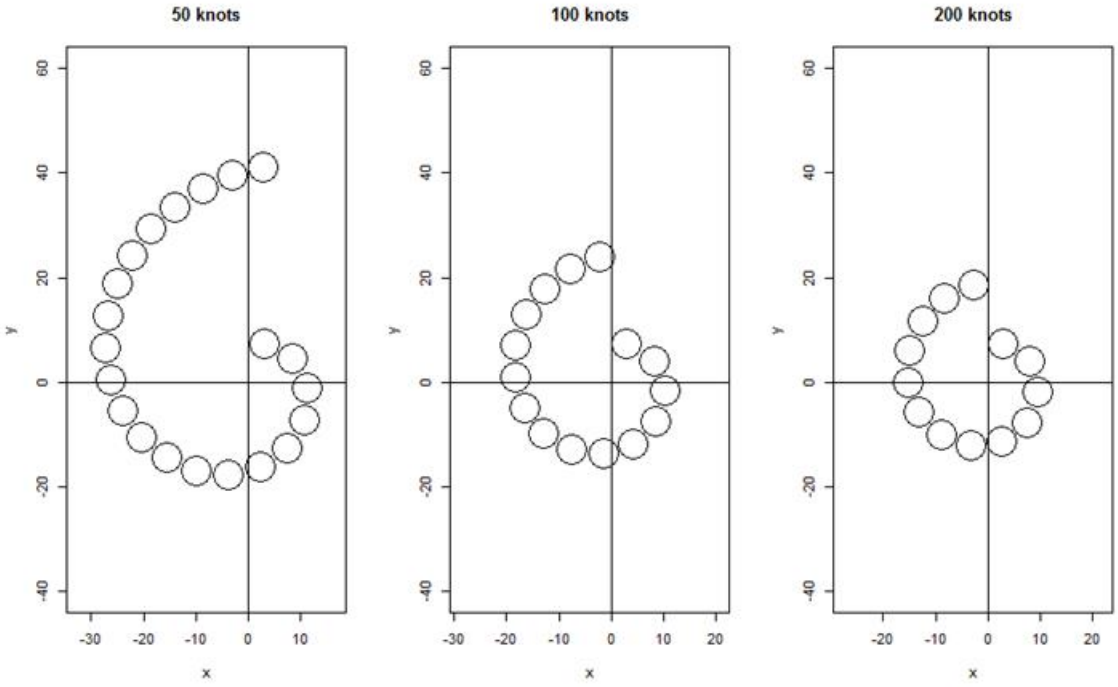

Figure 4: Dipping Patterns for Varying Helicopter Speeds (V = 50,100,200 knots)

The marginal effect of speed is demonstrated in the number of dips and the time it would take the helicopter to complete a full (360^{o}) spiral. See Figure 5. From the top plot in Figure 5 we see that as the speed of the helicopter increases the flat parts of the plot become longer. That is, the sensitivity of the number of dips to changes in speed decreases as the helicopter travels faster. The bottom plot shows that the effect of helicopter speed on the time to complete a full spiral is strictly monotone decreasing – as one would expect. The discontinuities in the plot, which are aligned with the jumps in the upper plot, correspond to unit decreases in the number of dips.

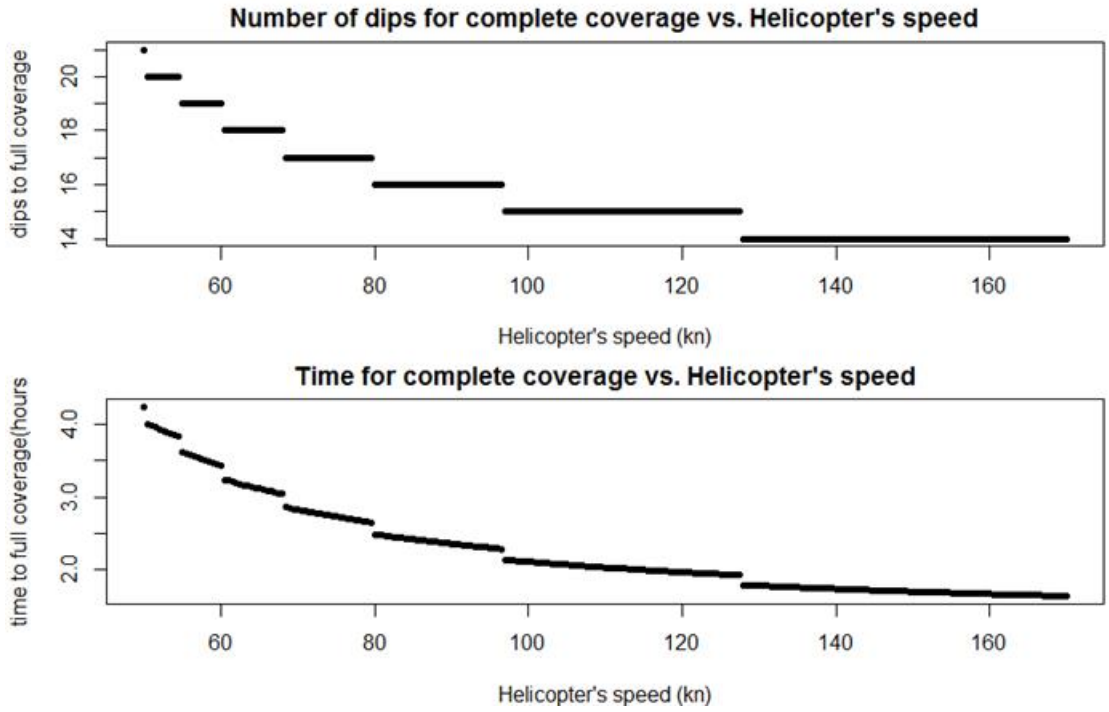

Figure 5: Number of Dips and Time to Complete a Search as a Function of Helicopter Velocity

Arrival Time (T_1) and Dipping Time (τ_D)

The decision to dispatch the search helicopter – the "go/no-go" decision – is crucially affected by the time T_1 it takes the helicopter to arrive at the first dipping point. For a given cruising speed of the helicopter, the arrival time is determined by the distance from the take-off site to the datum. Even if unrealistically we assume limitless endurance for the helicopter, that is, it could always complete a full spiral, the effect of arrival time on the shape of the spiral is quite significant, as shown in Figure 6.

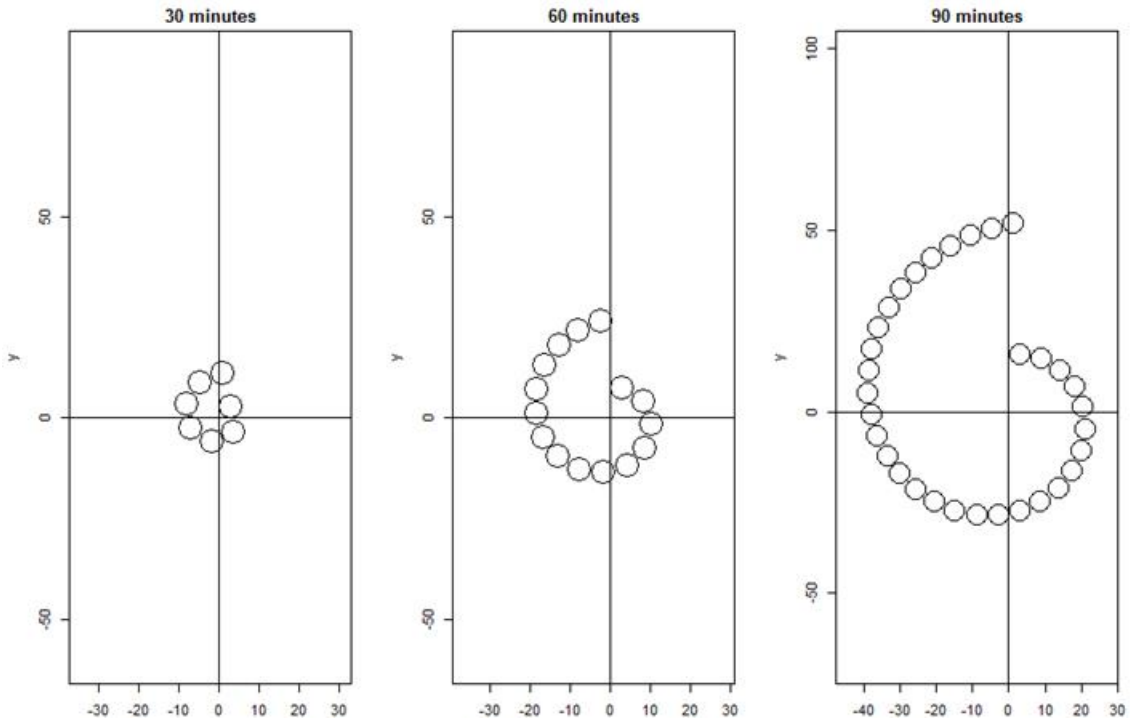

Figure 6: Dipping Pattern for T_1 = 30, 60 and 90 min

With limited endurance the effect of lower speed becomes even more significant; slower speeds directly create larger spirals (see Figure 4) and therefore more dips are needed for a given coverage, but slower speeds also increase T_1, which further increases the size of the spiral.

Similar effects occur when we vary the time it takes to execute a dip, as shown in Figure 7. As one would expect, longer dipping times generate bigger spirals but, surprisingly, while there is barely any difference between 2.5- and 5-minute dips, there is a significant change between 5- and 10-minute dips.

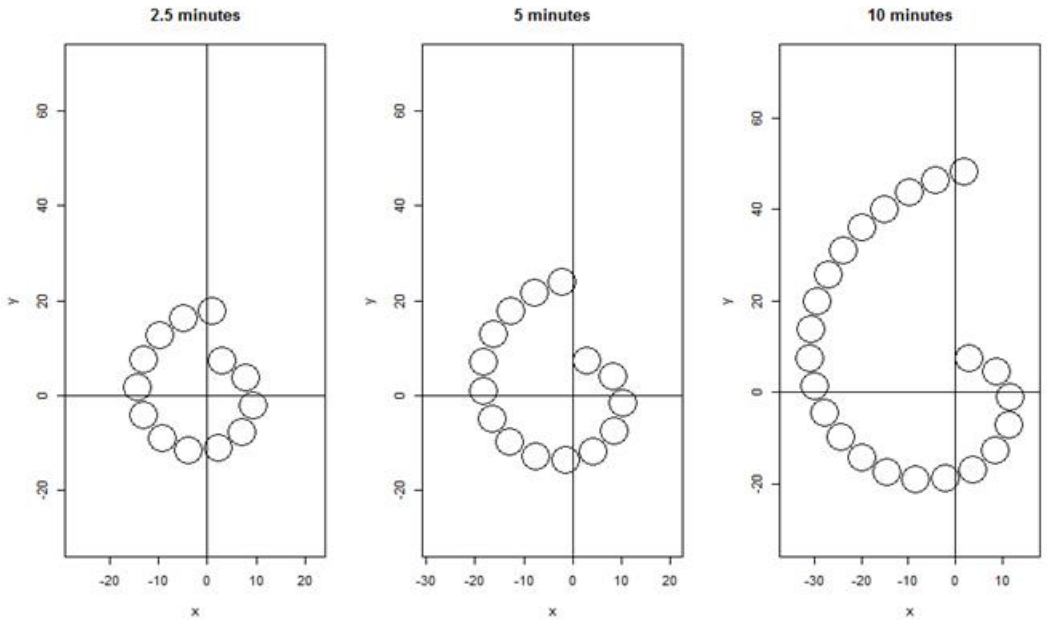

Figure 7: Dipping Pattern for τ_D = 2.5, 5 and 10 min

Detection Radius (*R*)

Figure 8 demonstrates the significant effect of the dipper's detection range.

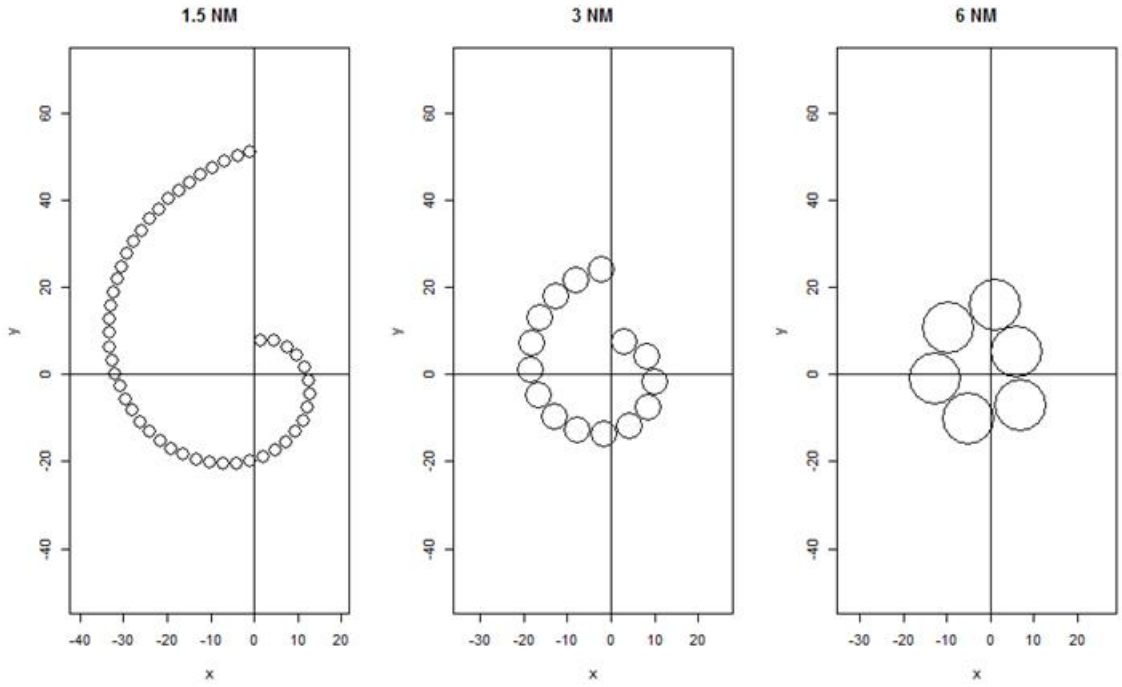

Figure 8: Dipping Pattern for *R* = 1.5, 3 and 6 nm

We observe that doubling the detection range from 1.5 miles to 3 miles reduces the number of dips by more than a factor 3. The effect of detection range on the number of dips and duration of a complete search appears in Figure 9.

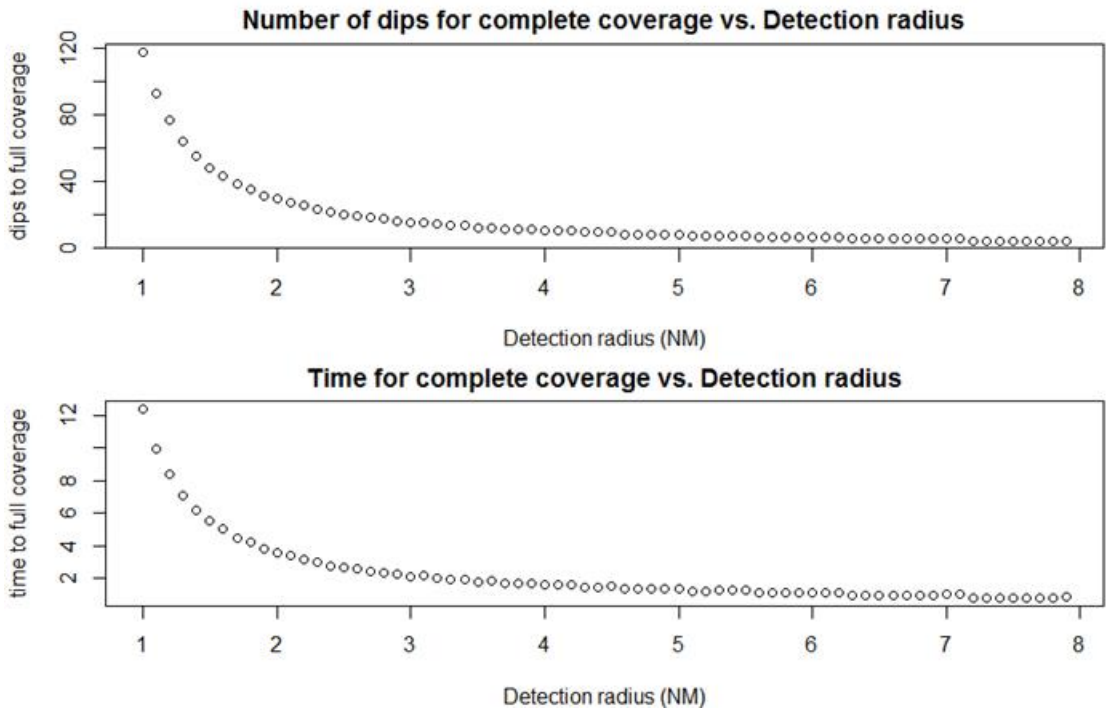

Figure 9: Number of Dips and Search Time for Varying Detection Ranges

As observed above, for small detection ranges (e.g., less than 1.5 mile) the effect of marginal improvement in range is super-linear, which is not the case for larger detection ranges where the marginal effect is negligible.

Submarine's Speed (U)

The submarine's speed is the only parameter that is not controllable by the searcher. As observed from Figure 10, the submarine's speed has a significant impact on the dipping pattern; doubling the speed of the sub from 8 knots (base case) to 16 knots results in more than quadrupling the number of required dips to

complete a spiral. For comparison, reducing the helicopter speed from 100 knots (base case) to 50 knots increases the number of dips by less than 30%.

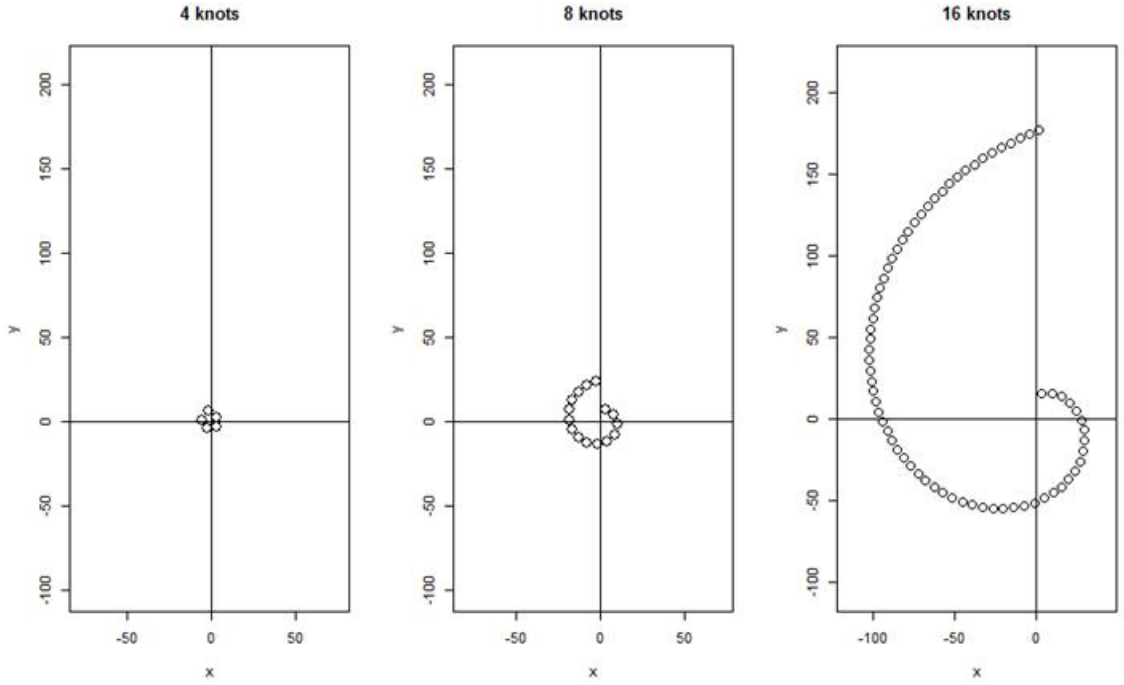

Figure 10: Dipping Pattern for U = 4, 8 and 16 knots.

In reality the searcher will not know exactly the submarine speed, only an estimate based on intelligence sources. The results reported above hold even when there is some uncertainty about the actual speed as long as the velocity error produces locational errors within the detection range of the dipper over the course of the search period.

6. PARTIAL INFORMATION ABOUT SUB'S BEARING

Thus far we assume that that the searcher has no information about the sub's bearing and therefore each direction of movement of the sub is taken to be equally likely. In some situations, however, additional information about the sub's bearing may be available and could be utilized to improve the effectiveness of the search. Suppose that the bearing of the submarine may be in one of three possible wedges of the LoU having angular sizes α, β and γ, $\alpha + \beta + \gamma \leq 360^{\circ}$, with probabilities q, p and $1 - p - q$, respectively. See Figure 11. The direction within a wedge is uniformly distributed, which implies that the

optimal dipping pattern within each wedge is derived from Theorem 1, and manifested by a partial spiral of tangential dips.

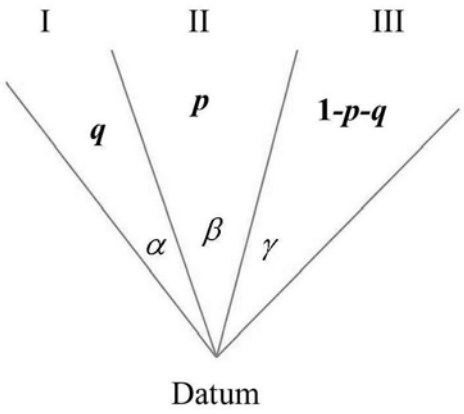

Figure 11: Bearing in One of Three Wedges

The question now is in what order to search the wedges. If the wedges are searched sequentially – I→II→III or III→II→I – then the dipping pattern is a spiral that starts on the left ray of wedge I or the right ray of wedge III, respectively. Otherwise, the helicopter has to "hop" over wedges and the dipping pattern is no longer a contiguous spiral. For example, if the search order is II→I→III then the helicopter starts the dipping at a point on the right ray of the middle wedge (II) and spirals towards the left ray of I. Once it reaches that ray, it flies back to a certain point, farther away on the right ray of II and resumes the search towards the right ray of III. See Figure 12. Note that unlike the continuous searches described for the cases I→II→III or III→II→I, in this search pattern there is some wasted "lull" time when the helicopter moves from wedge I to wedge III (the thin arrow in Figure 12). The objective is to minimize the expected time to detection and therefore such discontinuous dipping patterns are possible if, for example, $p > q >> 1 - p - q$.

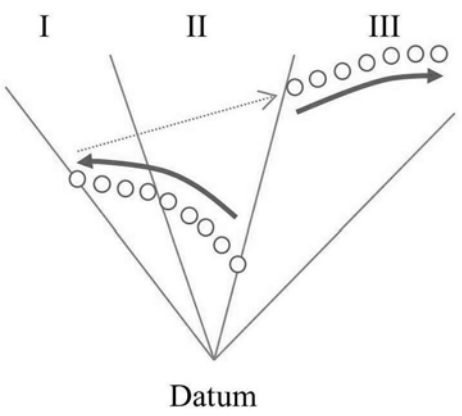

Figure 12: Dipping Pattern for II → I → III

There are six possible orders of searching the wedges:

1. I→II→III,
2. I→III→II,
3. II→I→III,
4. II→III→I,
5. III→I→II,
6. III→II→I.

Recall that our objective is to determine the search order that minimizes the expected time to detection. For each one of the six search orders, there are values of *p* and *q* for which the order is optimal. Figures 13 to 15 present the (*p*,*q*) region in which each order is optimal. The computational details for generating these figures appear in (Ben Yoash, 2016).

Figure 13 presents the case where $\alpha = \beta = \gamma = 30^{\circ}$ and the velocity ratio between the helicopter and the sub is $S = \frac{V}{U} = 10$. Each region is labeled with the number corresponding to the search order presented above. For example, region 1 contains all the (*p*,*q*) values for which the wedges search order is $I \to II \to III$.

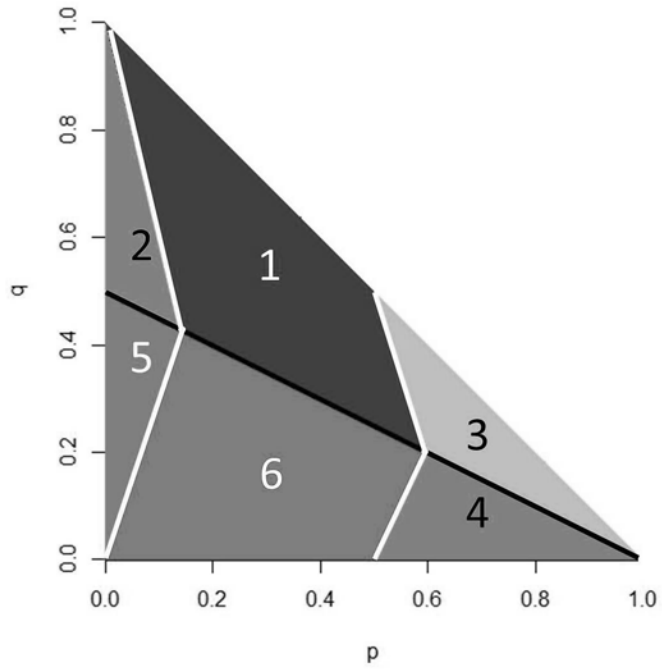

Figure 13: Three Wedges Model, $\alpha = \beta = \gamma = 30^{\circ}, S = 10$.

We see that the larger p is (probability that the submarine is in wedge II), the more likely we are to start in that middle wedge (search orders 3 and 4). If q (probability of the submarine in the wedge I) is relatively large, then it is more likely that the search will start at wedge I (patterns 1 and 2).

Figure 14 demonstrates the effect of varying the sizes of the two side wedges – the angles α and γ - on the optimal order. We vary them together, keeping the two other parameters constant ($\beta = 30^{\circ}, S = 10$).

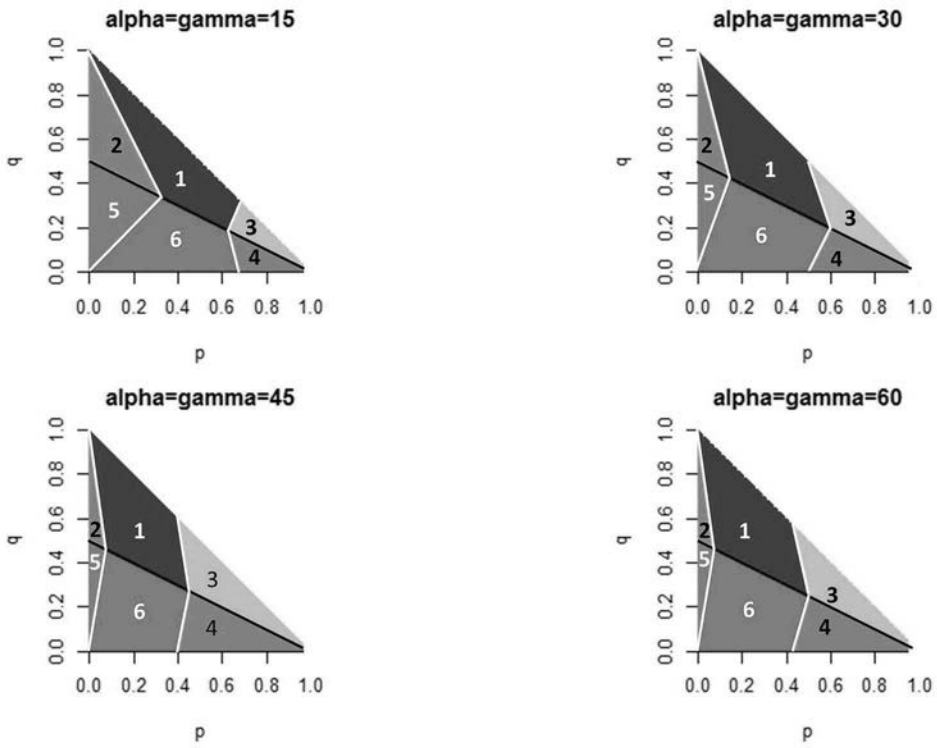

Figure 14: Three Wedges Model, $S = 10, \beta = 30, \alpha$ and γ Varied.

We see that increasing the angles of the side wedges decreases the regions of (*p*,*q*) where patterns 2 and 5 – orders in which the center wedge is searched last. Although this seems counterintuitive, the explanation is that searching the center wedge last means that the helicopter has to fly over a side wedge, which has already been searched, back to the center. This wasted flying time increases as the side wedge becomes wider. We also see that regions 3 and 4 increase, that is, starting the search at the center wedge becomes more common, when the side wedges increase in size. This happens because wider wedges imply lower probability per unit angle, which make them less attractive in terms of "bang-for-the-dip" – the expected reward from a dip. We notice however that for side wedges wide enough the changes are marginal (e.g., see the plots for 45^o and 60^o.)

Last we examine the sensitivity of the search order to the speed ratio *S* between the helicopter and the submarine. We assume $\alpha = \beta = \gamma = 30^\circ$ throughout. Figure 15 depicts this sensitivity:

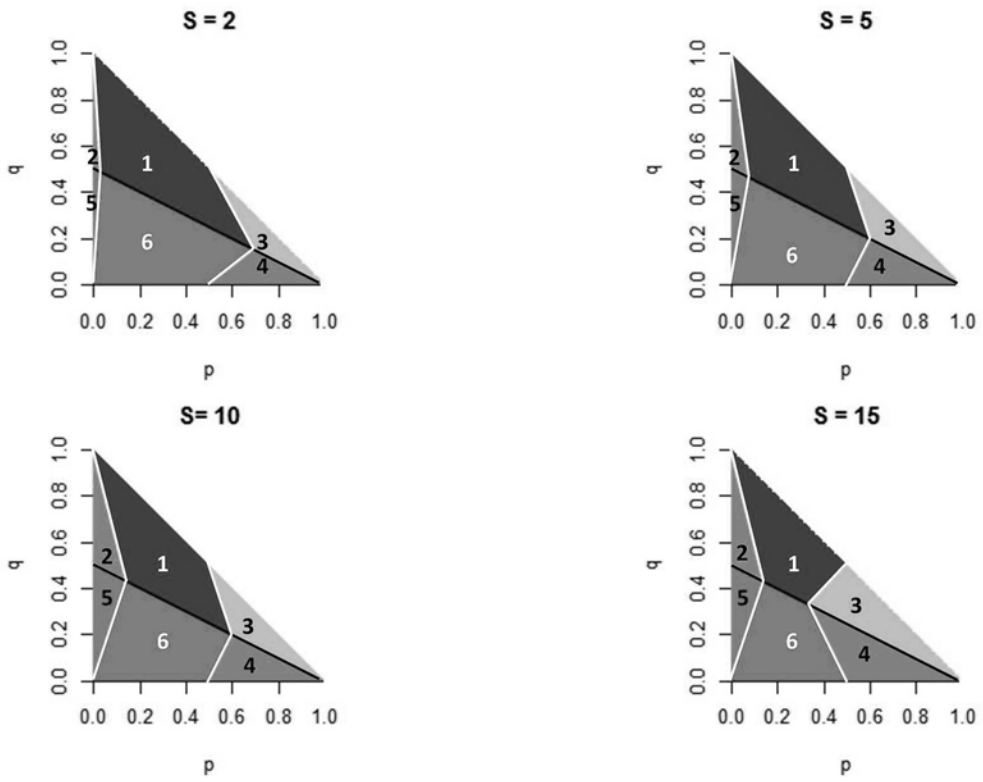

Figure 15: Three Wedges Model, $\alpha = \beta = \gamma = 30^{\circ}, S$ Varied.

Clearly, as the speed ratio increases, patterns 1 and 6 become less common and patterns 2, 3, 4, and 5 become more common. Orders 1 and 6 are the only search patterns that do not involve "hopping" over wedges (i.e., patterns $I \to II \to III$ and $III \to II \to I$). The faster the helicopter flies, the less significant is the time loss for jumping over wedges.

7. CONCLUSIONS

The US Navy MH-60R helicopter may be equipped with dipping sonar for detecting and localizing adversaries' submarines. This discrete search pattern is different from more common continuous searches. In this paper, we present an analysis of the optimal dipping frequency. We primarily focus on the deterministic submarine velocity scenario and derive an optimal dipping pattern: the optimal next dipping location is the closest point that produces a disjoint dip. We investigate the effect of various operational and physical parameters on the characteristics of the dipping pattern. We observe that temporal parameters – time to arrival to the datum and velocity of the submarine – have significant effect on the dipping pattern and the time to complete a full coverage (spiral) of the submarine location. We also examine the case where the submarine velocity is a random variable. Disjoint dips are not necessarily optimal in this scenario when the helicopter arrives on station quickly. However, for most realistic parameter values, a disjoint dipping strategy should perform near optimally. Future work could consider more realistic detection functions and more complex target dynamics, such as counter-detection.

ACKNOWLEDGEMENT
This paper is based on the Master's Thesis of Roey Ben Yoash (first author).

REFERENCES

Baston, V.J. and Bostock, F.A., 1989. A one-dimensional helicopter-submarine game. *Naval Research Logistics*, 36(4), pp. 479-490.

Ben Yoash, R.. 2016. *Anti-Submarine Warfare Search Models*. Naval Postgraduate School, Monterey, CA.

Chuan, E. 1988. *A helicopter submarine search game*. Master thesis, Naval Postgraduate School, Monterey, CA.

Danskin, J.M. 1968. A helicopter versus submarine search game. *Operations Research*, 16(3), pp. 509-517.

The Free Dictionary by Farlex, s.v. *dipping sonar*, retrieved June 7, 2016, http://encyclopedia2.thefreedictionary.com/dipping+sonar

Global Security, 2016. *ASW Helicopters,* http://www.globalsecurity.org/military/systems/aircraft/rotary-asw.htm. Accesses on 27 November 2016.

Haley, B.K. and Stone L.D. 1980. *Search Theory and Applications.* Plenum Press, New York.

Kim, K-M. and Lee, S-H. 2012. Approximating the Poisson Scan and ($\lambda-\sigma$) acoustic detection model with a Random Search formula. *Computers and Industrial Engineering* 62(3), pp. 777-783.

Marsden, J.E. and Hoffman, M.J., 1993. *Elementary classical analysis*. Macmillan.

Shephard R.W., Hartley D.A., Haysman P.J., Thorpe L. and Bathe M.R. 1988. *Applied Operations Research.* Plenum Publishing Corporation, New York.

Stone, L.D. 1975. *Theory of Optimal Search.* Academic press, New York.

Soto, A. 2000. *The Flaming Datum problem with varying speed*. Master thesis, Naval Postgraduate School, Monterey, CA.

Thomas, L.C. and Washburn, A.R., 1991. Dynamic search games. *Operations Research*, 39(3), pp.415-422.

Washburn A. 1980. *Expanding area search experiments*, Naval Postgraduate School, Monterey, CA.

Washburn, A. R., and Hohzaki, R. and 2001. The diesel submarine flaming datum problem. *Military Operations Research,* 6(4), pp. 19-30.

Washburn, A. 2002. *Search and Detection*, 4th edition. Institute for Operations Research and the Management Sciences, Linthicum, MD.

Weisstein, E.W. 2017. *Circle-Circle Intersection*. From MathWorld--A Wolfram Web Resource. http://mathworld.wolfram.com/Circle-CircleIntersection.html

APPENDIX A: Proof of Theorem 1

We first provide additional background and notation in Section A.1, before proceeding with the proof in Section A.2. We present the mathematical representation for the optimal dipping pattern at the end of Section A.1.

Section A.1 Background

We define the optimal dipping pattern as the one that, given a limited number of dips (because of limited flight endurance), maximizes the probability of detecting the submarine. Since we assume that we know the speed U of the submarine, the location of uncertainty at time T is a circumference of a circle with radius $T \times U$. Since the size of the circumference is growing with time, we analyze the problem using coverage angles. Absent any knowledge regarding the bearing of the submarine, we assume any direction is equally likely, that is, the direction of the submarine is uniformly distributed between 0° and 360°.

Given a particular dip (not necessarily the first one) that occurs at time *T*, we compute the coverage angle α. See Figure A.1 for reference. The dip footprint D_P in Figure A.1 is the circle centered at the dip point with radius *R* (the dipper's detection range). The coverage angle α satisfies $\sin\left(\alpha/2\right) = \frac{R}{T \times U}$, so

$$\alpha = 2\sin^{-1}\left(\frac{R}{T \times U}\right),$$

where we assume the inverse sin function returns degrees.

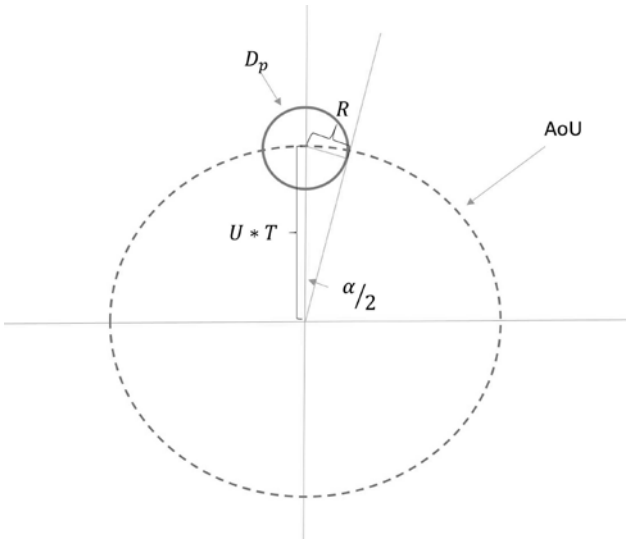

Figure A.1: Illustration of Coverage Angle α.

Since the movement direction of the submarine is uniformly distributed, the probability of detection by a dip that has no overlap with previous dips equals the coverage angle divided by 360. If the dip has overlap with previous dips, then the effective coverage of the current dip is its coverage α minus the overlap with the previous dips. Mathematically the detection probability of one dip at time T satisfies

$$P[\text{detection during dip at time } T] \le \frac{\alpha}{360} = \frac{\sin^{-1}\left(\frac{R}{T \times U}\right)}{180}.$$

The inequality follows because the dip at time at time T may overlap with previous dips. If there is no overlap, the detection probability is exactly $\alpha / 360$.

Obviously, larger effective coverage is equivalent to a higher detection probability. The question is what is the optimal way to dip? More precisely: given the current dip location P_i, what is the optimal next dip location P_{i+1}^*? We assert that Figure A.2 illustrates the answer to this second question.

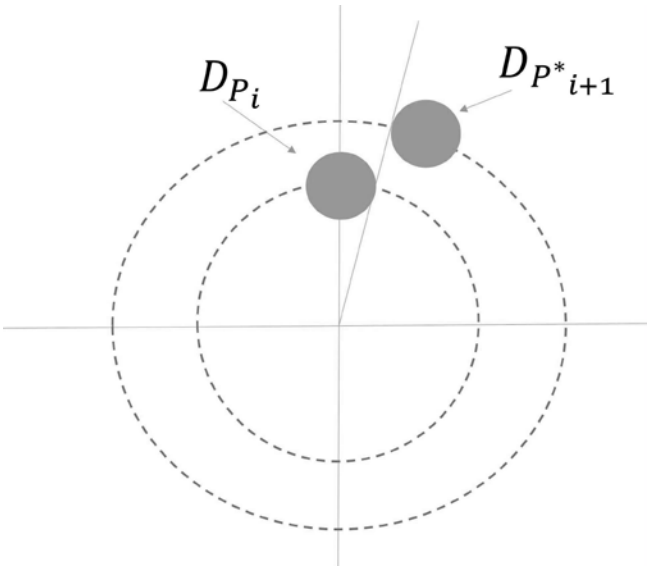

Figure A.2: Optimal Next Dipping Location P^*_{i+1}

Looking at Figure A.2, we claim that after dipping at point P_i the best next dipping point, P^*_{i+1}, would be a disjoint one. Moreover, point P^*_{i+1} is the closest possible disjoint dip. That is the dip footprint $D_{P^*_{i+1}}$ is tangent to the same tangent line of footprint D_{P_i} but "from the other side" (as shown in Figure A.2). We prove this in Section A.2 and provide a mathematical representation for P^*_{i+1} at the end of this section.

Before turning to the proof, we make a few observations and introduce additional notation. The *i*-th dip begins at time T_i at location P_i. The datum is determined at time 0, and time is measured since that event. We define P_i using a modified polar coordinate system: $P_i = (K_i, \theta_i)$, where $K_i = U \times T_i$ is the submarine's distance from the datum at the *i*-th dip, and θ_i is the angle, rooted at the datum, measured clockwise with respect to the *vertical* axis. Because the submarines velocity is known, the radial component K_{i+1} of P_{i+1} is uniquely determined and therefore to determine the next dipping location P_{i+1} (not necessarily optimal), we only need to specify θ_{i+1} (or, equivalently $\theta_{i+1} - \theta_i$). Once we know θ_{i+1} we can use velocity/distance/time calculations to determine when the helicopter will reach a

valid P_{i+1} along the ray defined by θ_{i+1} from the current dipping point P_i. This calculation yields T_{i+1} and hence $K_{i+1} = U \times T_{i+1}$. Consequently, specifying θ_{i+1} determines the actual next dipping point. More rigorous mathematical details appear in Section A.2.

Since we only need to determine the angle of the next dip, we first define $\omega_{i+1} = \theta_{i+1} - \theta_i$, which is the angle created by the previous dip, the datum, and the new dip, as illustrated in Figure A.3. We next define $f(\omega)$ as the effective coverage of a dip with angular difference ω.

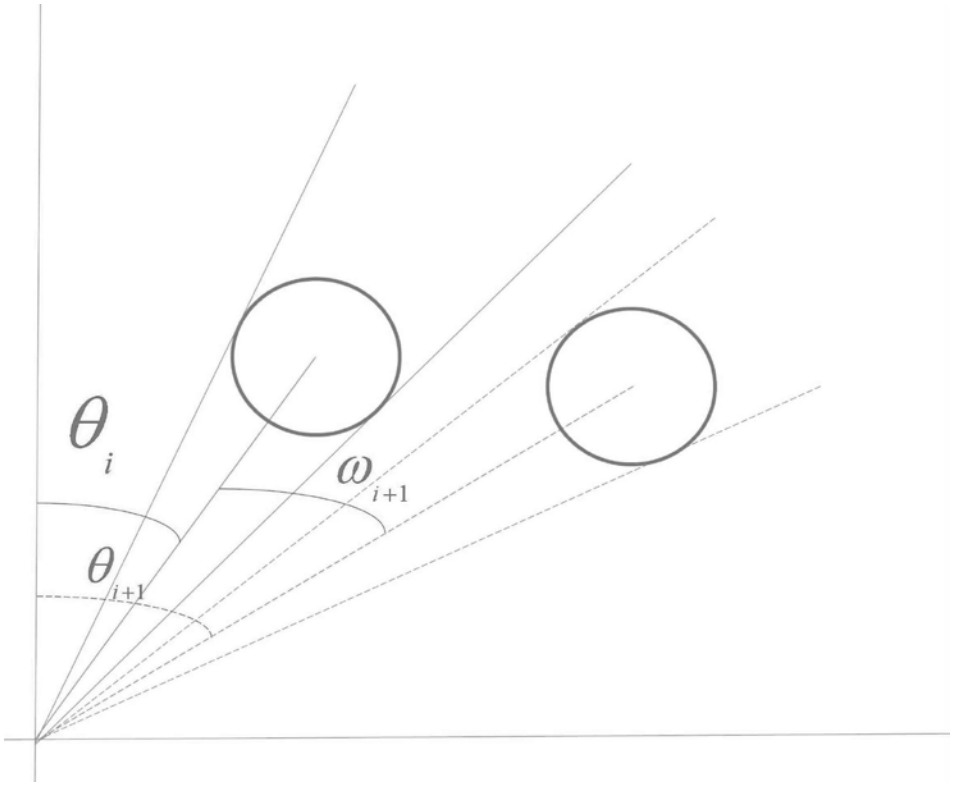

Figure A.3: Definition of ω.

If $\omega_{i+1} = 0$ then the helicopter's next location P_{i+1} lies on the same ray as P_i. P_{i+1} does not equal P_i even when $\omega_{i+1} = 0$ because there is a positive dipping time τ_D. Consequently, $f(0) = 0$ because dipping along the same ray as the previous dip will produce no additional coverage relative to the previous dip.

In most realistic scenarios the helicopter does not arrive to the datum fast enough to find the submarine with one dip at the datum, i.e., $R < K_1 = T_1 \times U$, where K_1 is the distance of the first dip from the datum and $\theta_1 = 0$ is its angle measured clockwise from the vertical axis. Subsequent dips occur in a clockwise fashion and hence the angles θ_i form a monotonically increasing series. The duration of a dip is τ_D and its location remains stationary throughout; the helicopter hovers over the dipping point.

We conclude this section by presenting the formulas we use to compute the optimal location of the next dip $P_{i+1}^* = (K_{i+1}^*, \theta_{i+1}^*)$ given current dip location $P_i = (K_i, \theta_i)$. These two equations simultaneously solve for displacement angle ω_{i+1}^* and the time of dipping T_{i+1}^*, which yields $K_{i+1}^* = U \times T_{i+1}^*$ and $\theta_{i+1}^* = \theta_i + \omega_{i+1}^*$.

$$\omega_{i+1}^* = \cos^{-1}\left(\frac{(U \times T_i)^2 + (U \times T_{i+1}^*)^2 - (V \times (T_{i+1}^* - T_i - \tau_D))^2}{2 \times U^2 \times T_i \times T_{i+1}^*} \right) \qquad \text{(A.1)}$$

$$\omega_{i+1}^* = \sin^{-1}\left(\frac{R}{T_i \times U} \right) + \sin^{-1}\left(\frac{R}{T_{i+1}^* \times U} \right) \qquad \text{(A.2)}$$

Equation (A.1) relates to time/distance calculations to ensure the searcher's next dip location is consistent with the submarine's radial location. Equation (A.2) guarantees that there is no overlap between dip *i*+1 and dip *i*: the two dips are disjoint. More details and the proof of optimality appear in the next section.

Section A.2 Proof of the Optimal Dipping Pattern

Our proof follows three steps:

1. Show that equations (A.1) and (A.2) mathematically define our desired next dipping point P_{i+1}^*: the closest disjoint dip.
2. Show that the effective coverage function $f(\omega)$ is continuous.
3. Show that P_{i+1}^* is the optimal next dip via contradiction.

We first relate the current position P_i to the next dip position P_{i+1} (not necessarily optimal) using the Law of Cosines as illustrated in Figure A.4:

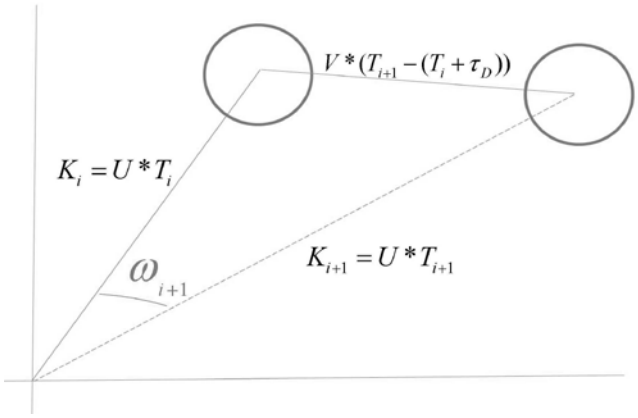

Figure A.4: Relating ω_{i+1} to T_{i+1}.

The distance from the datum to the current dipping point, P_i, is $K_i = U \times T_i$, and the distance from the datum to the next dipping point, P_{i+1}, is $K_{i+1} = U \times T_{i+1}$. The helicopter departs from P_i at time $T_i + \tau_D$ after finishing the dip and arrives to P_{i+1} at time T_{i+1}, and therefore the distance between P_i and P_{i+1} is $V \times (T_{i+1} - (T_i + \tau_D))$, where V is the helicopter's velocity. Using the Law of Cosines (assuming $\omega_{i+1} < 180^\circ$), we have the following relationship:

$$(V \times (T_{i+1} - T_i - \tau_D))^2 = (U \times T_i)^2 + (U \times T_{i+1})^2 - 2 \times U^2 \times T_i \times T_{i+1} \cos(\omega_{i+1}). \quad \text{(A.3)}$$

Equation (A.3) defines an implicit function of T_{i+1} with respect to ω_{i+1}. T_{i+1} is a continuous function of ω_{i+1} by the Implicit Function Theorem (see Chapter 7.2 of Marsden and Hoffman(1993)). The only conditions we need are $T_i, T_{i+1} > 0$, which follow by assumption, and then T_{i+1} is continuous in ω_{i+1} for all $0 < \omega_{i+1} < 180$.

Solving equation (A.3) for ω_{i+1} produces equation (A.1).

$$\omega_{i+1} = \cos^{-1}\left(\frac{(U \times T_i)^2 + (U \times T_{i+1})^2 - (V \times (T_{i+1} - T_i - \tau_D))^2}{2 \times U^2 \times T_i \times T_{i+1}} \right).$$

Thus using equation (A.3) (or (A.1)), the angle differential ω_{i+1}, uniquely determines the time of the next dip such that the radial position of the helicopter corresponds to the radial position of the submarine.

Next we derive an explicit expression for the effective coverage function $f(\omega)$. If $g(\omega_{i+1})$ denotes the overlap between the two dips, then

$$f(\omega_{i+1}) = \alpha - g(\omega_{i+1}) = 2 \times \sin^{-1}\left(\frac{R}{T_{i+1} \times U}\right) - g(\omega_{i+1}) \qquad \text{(A.4)}$$

Recall that the overlap is the angle between the left tangent to $D_{P_{i+1}}$ and the right tangent to D_{P_i}, as shown in Figure A.5.

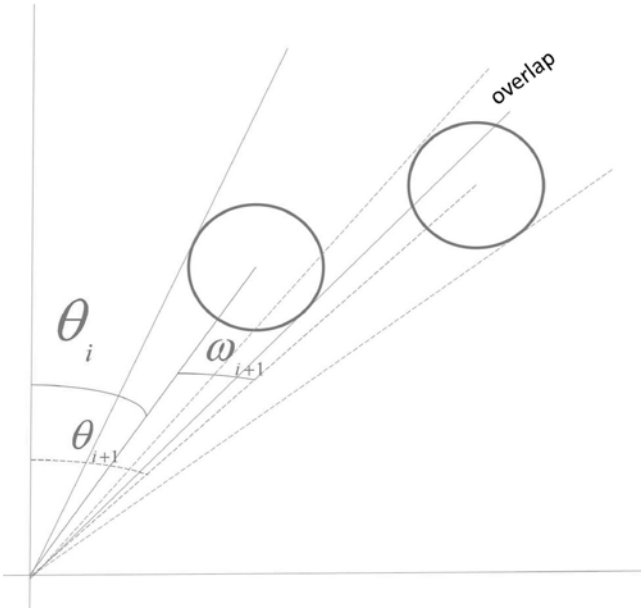

Figure A.5: Overlap Calculation.

The angle between the vertical axis and the right tangent to D_{P_i} can be expressed as

$$\theta_i + \frac{\alpha_i}{2} = \theta_i + \sin^{-1}\left(\frac{R}{T_i \times U}\right),$$

and the angle between the vertical axis to the left tangent to $D_{P_{i+1}}$ is

$$\theta_{i+1} - \frac{\alpha_{i+1}}{2} = \theta_{i+1} - \sin^{-1}\left(\frac{R}{T_{i+1} \times U}\right).$$

The overlap is the difference between these two angles, that is,

$$g(\omega_{i+1}) = \theta_i + \sin^{-1}\left(\frac{R}{T_i \times U}\right) - \theta_{i+1} + \sin^{-1}\left(\frac{R}{T_{i+1} \times U}\right)$$
$$= \theta_i - \theta_{i+1} + \sin^{-1}\left(\frac{R}{T_i \times U}\right) + \sin^{-1}\left(\frac{R}{T_{i+1} \times U}\right),$$

which simplifies to

$$g(\omega_{i+1}) = -\omega_{i+1} + \sin^{-1}\left(\frac{R}{T_i \times U}\right) + \sin^{-1}\left(\frac{R}{T_{i+1} \times U}\right) \qquad \text{(A.5)}.$$

Our candidate for the optimal next position P_{i+1}^* is the closest dip to P_i with no overlap, and hence $g(\omega_{i+1}^*) = 0$. Therefore, to derive condition (A.2), we set (A.5) to 0. Examination of (A.4) and (A.5) reveals that $f(\omega_{i+1})$ is a continuous function. Both $\frac{R}{T_i \times U}$ and $\frac{R}{T_{i+1} \times U}$ are positive and less than 1 by assumption. Furthermore, T_{i+1} is a continuous function of ω_{i+1} (see discussion following (A.3) above). Consequently $f(\omega_{i+1})$ is continuous by the continuity of function composition (see Chapter 4.3 of Marsden and Hoffman(1993)).

Now that we have derived conditions (A.1) and (A.2), and showed that $f(\omega_{i+1})$ is continuous, we proceed to prove the result in Theorem 1 by contradiction. Suppose location $\tilde{P}_{i+1}$ is a better location for the next dip than our proposed location P_{i+1}^*, which satisfies equations (A.1) and (A.2). That is $\tilde{P}_{i+1}$ produces a higher effective coverage than P_{i+1}^*. P_{i+1}^* "shares" a tangent with the current location P_i (see Figure A.2). Therefore, $\tilde{P}_{i+1}$ must be closer to the datum than P_{i+1}^* because a location farther away will obviously have a smaller coverage. We claim that $\tilde{\omega}_{i+1} < \omega_{i+1}^*$ must hold. Because $\tilde{P}_{i+1}$ lies closer to the datum than P_{i+1}^*, it follows that $\tilde{K}_{i+1} < K_{i+1}^* \Rightarrow \tilde{T}_{i+1} < T_{i+1}^*$ (see Figure A.4). Condition (A.1) ensures that pairs of (ω_{i+1}, T_{i+1}) produce valid dipping points P_{i+1}. Inspection of (A.1) reveals that ω_{i+1} is an increasing function in T_{i+1} as long as $T_{i+1} > T_i + \tau_D$. Therefore, $\tilde{T}_{i+1} < T_{i+1}^*$ implies $\tilde{\omega}_{i+1} < \omega_{i+1}^*$.

If indeed $\tilde{P}_{i+1}$ covers a larger angular section than P^*_{i+1}, we next argue that there must exist a valid dipping point P_j that is reachable by the helicopter in time to dip and has the same effective coverage as P^*_{i+1}, as shown by the middle circle in Figure A.6.

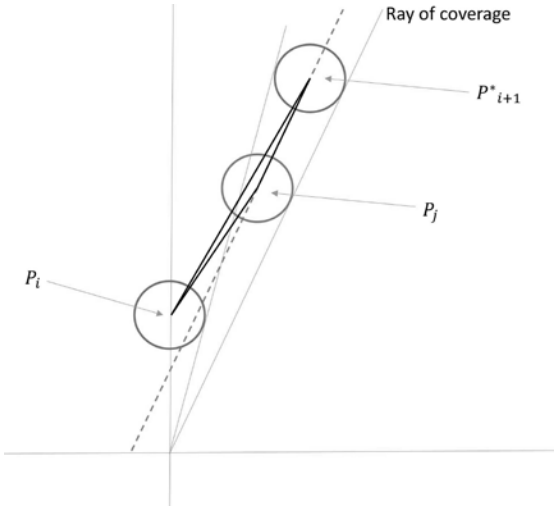

Figure A.6: Illustration of the Contradiction.

We prove the existence of point P_j using the Intermediate Value Theorem (see Chapter 4.5 of Marsden and Hoffman(1993)). As argued above, the effective coverage function $f(\omega_{i+1})$ is continuous. We discussed in Section A.1 that $f(0) = 0 \leq f(\omega^*_{i+1})$ (coverage cannot be negative), and by definition, if location $\tilde{P}_{i+1}$ is a better location to dip than P^*_{i+1}, then $f(\tilde{\omega}_{i+1}) > f(\omega^*_{i+1})$. Finally, we showed $\tilde{\omega}_{i+1} < \omega^*_{i+1}$ in the previous paragraph. Putting these pieces together with the Intermediate Value Theorem, there is an ω_j (and therefore P_j) for which $f(\omega_j) = f(\omega^*_{i+1})$ and $0 < \omega_j < \tilde{\omega}_{i+1} < \omega^*_{i+1}$. This implies that P_j is closer to the current dipping point than P^*_{i+1} and produces the same effective coverage. Figure A.7 illustrates the logic graphically.

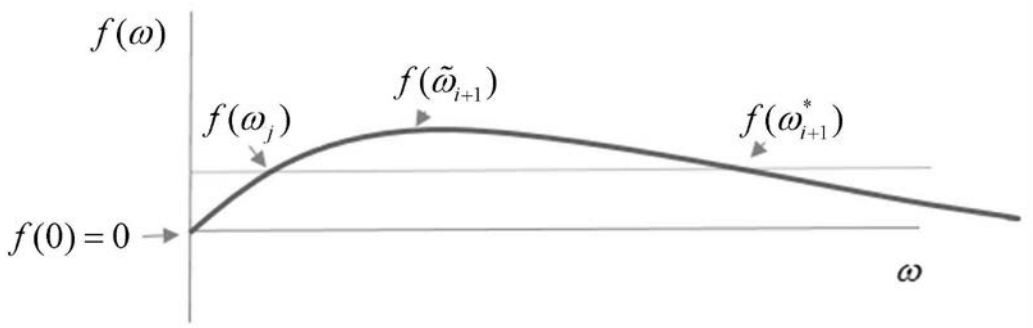

Figure A.7: Intermediate Value Theorem.

The angular coverage of D_{P_j} overlaps with the angular coverage of D_{P_i} because D_{P_j} is closer to D_{P_i} than $D_{P^*_{i+1}}$ (See Figure A.6). Consequently, to generate the same effective coverage, $D_{P^*_{i+1}}$ and D_{P_j} must both be tangent (on the right-hand side) to the same ray from the datum. This follows because the effective coverage is the angle created by the right tangent to D_{P_i} and the right tangent to both $D_{P^*_{i+1}}$ and D_{P_j}. We call the later ray the "ray of coverage" (See Figure A.6). From the geometry displayed in Figure A.6 it follows that the line through P^*_{i+1} and P_j (dotted line in Figure A.6) is parallel to the "ray of coverage" at a distance *R* away from the ray. We now show that the existence of P_j leads to a contradiction. We first reintroduce the parameter *K*, which is the distance from the datum to the dipping point of interest. We next define $Dist_{i,i+1}$ as the distance between P_i to P^*_{i+1}. We note that $Dist_{i,i+1} = V \times \left(\frac{K^*_{i+1} - K_i}{U} - \tau_D \right)$ is the distance the helicopter travels while the submarine moves between the two radii K_i and K^*_{i+1}. Similarly, we define $Dist_{i,j} = V \times \left(\frac{K_j - K_i}{U} - \tau_D \right)$ as the distance between P_i and P_j. The distance $Dist_{j,i+1}$ between P_j and P^*_{i+1} can be found by considering the dotted line in Figure A.6, which is parallel to the "ray of coverage." That is, $Dist_{j,i+1} = K^*_{i+1} - K_j$. We now observe that

$$
\begin{aligned}
Dist_{i,j} + Dist_{j,i+1} &= V \times \left(\frac{K_j - K_i}{U} - \tau_D \right) + (K^*_{i+1} - K_j) \\
&< V \times \frac{K_j - K_i}{U} + V \times \frac{(K^*_{i+1} - K_j)}{U} - V\tau_D \\
&= \frac{V}{U}[(K_j - K_i) + (K^*_{i+1} - K_j)] - V\tau_D \\
&= \frac{V}{U}(K^*_{i+1} - K_i) - V\tau_D \\
&= V \times \left(\frac{K^*_{i+1} - K_i}{U} - \tau_D \right) \\
&= Dist_{i,i+1}
\end{aligned}
$$

The inequality part of the above expression follows from the fact that $V > U$; the helicopter moves faster than the submarine. The inequality implies that we found a path from P_i to P^*_{i+1} that is shorter than $Dist_{i,i+1}$, contradicting the fact that $Dist_{i,i+1}$ is the shortest distance from P_i to P^*_{i+1}. We conclude that there is no location $\tilde{P}_{i+1}$ that provides higher effective coverage than P^*_{i+1}, and the theorem is proved.

$\theta^*_{i+1} = \theta_i + \omega^*_{i+1}$

APPENDIX B: Proof of Theorem 2

We assume the searcher makes two dips. The searcher arrives at time T_1 and, without loss of generality, dips at the position defined by angular component $\theta_1 = 0$ and radial component $K_1 = U \times T_1$. As in Appendix A, we measure the angular component θ_i clockwise from the vertical axis.

For the second dip, the closest disjoint dipping location is defined by $K_2^D = U \times T_2^D$ and $\theta_2^D = \theta_1 + \omega_2^D$, where T_2^D and ω_2^D are the solutions to the set of simultaneous equations defined by (A.1) and (A.2). Given these parameters, the overall detection probability for this disjoint 2-dip pattern is

$$P_{disjoint}[detect] = \frac{(\alpha_1 + \alpha_2^D)q}{360},$$

where

$$\alpha_1 = 2\sin^{-1}\left(\frac{R}{T_1 \times U}\right), \qquad \alpha_2^D = 2\sin^{-1}\left(\frac{R}{T_2^D \times U}\right).$$

We contrast the disjoint 2-dip pattern with the other extreme: a complete overlap 2-dip pattern. If the 2nd dip completely overlaps the first, the searcher wants the 2nd dip to occur as quickly as possible (to maximize the size of the overlap). We define T_2^O and ω_2^O to represent the position of the closest overlap dipping location. This overlap position occurs when $\theta_2^O = \theta_1 = 0$ and $\omega_2^O = 0$. See Figure A.4 for reference. In this case we have a closed form expression for the time of the 2nd dip as equation (A.1) simplifies considerably: $T_2^O = T_1 + \frac{\text{V}}{\text{V-U}}\tau_D$. The detection probability using this complete overlap 2-dip pattern is

$$P_{overlap}[detect] = \frac{(\alpha_1 - \alpha_2^O)q + \alpha_2^O(1-(1-q)^2)}{360},$$

where

$$\alpha_1 = 2\sin^{-1}\left(\frac{R}{T_1 \times U}\right), \qquad \alpha_2^O = 2\sin^{-1}\left(\frac{R}{T_2^O \times U}\right).$$

Comparing $P_{overlap}[detect]$ to $P_{disjoint}[detect]$, the searcher should implement an overlap strategy if $\alpha_2^O(1-q) > \alpha_2^D$. Below we present a numerical example where this condition holds and hence the disjoint dipping strategy is suboptimal.

- V = 7 kts
- U = 6 kts
- R = 4.5nm
- $T_1 = 1$ hour
- $\tau_D = 1$ minute

- $q = 0.4$

For the above parameters $P_{overlap}[detect] = 0.164$ and $P_{disjoint}[detect] = 0.129$. This is not a realistic scenario as the searcher velocity *V* will likely be much higher than the target velocity *U*.

APPENDIX C: Proof of Theorem 3

In Section C.1 we derive the formulas for computing the overlap and detection probabilities of two successive dips. In Section C.2 we present examples where overlapping dips are optimal.

Section C.1 Overlap Between Two Successive Dips

Since we only need to show a counterexample to prove disjoint dips are not necessarily optimal, we assume that the helicopter makes just two dips. The helicopter executes its first dip at time T_1 at distance ρ_1 from the datum, with $\rho_1 \le \rho(T_1) = U_{max} T_1$. Without loss of generality we assume that the first dip location lies on the vertical axis at $(0, \rho_1)$. To avoid cumbersome bookkeeping, we further assume that T_1 and ρ_1 satisfy $R \le \rho_1 \le (\rho(T_1) - R)$. That is, the first dip is entirely contained within the upper part of the containment circle. See Figure C.1 for an illustration. The solid $-\square-$ circle in Figure C.1 represents the footprint of the first dip at time T_1, and the dotted $\cdots\square\cdots$ circle is the boundary of the containment circle: a circle of radius $\rho(T_1)$. Because the heading and velocity are uniformly distributed within the speed circle of radius U_{max} kts, the location of the submarine at time T_1 is uniformly distributed within the circle of containment of radius $\rho(T_1)$

nm. Therefore, the detection probability of the first dip is $\frac{R^2}{\rho^2(T_1)}$.

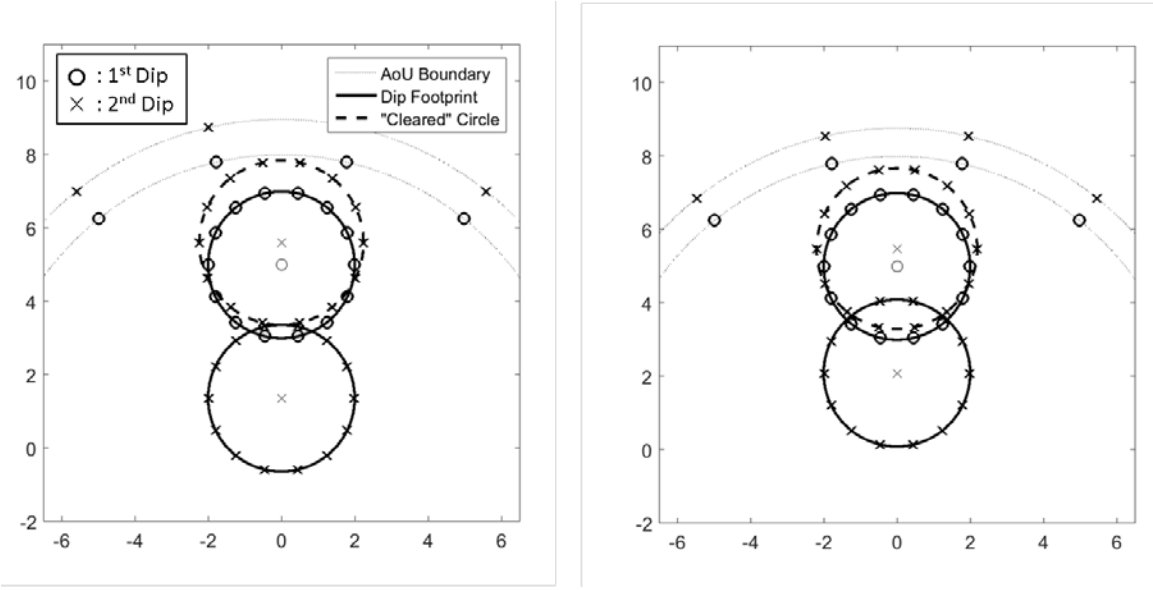

Figure C.1: Disjoint dips (left panel) vs Overlapping dips (right panel).

The second dip occurs at time $T_2 = T_1 + \Delta t$. The first dip "clears" from the speed-circle all velocity/heading combinations that lie within a circle centered at $(0, \rho_1 / T_1)$ with radius R / T_1 (units in speed circle are in kts). Because the submarine does not change heading or velocity, the velocity/heading combinations in the cleared circle can be eliminated from future consideration (assuming the first dip does not detect the target). Any additional search of those combinations produces overlap and redundant search effort.

In real-space, the cleared circle at time T_1 has center $(0, \rho_1)$ and radius *R*. At time $T_2 = T_1 + \Delta t$, this cleared circle has expanded in real-space to a radius of $R\left(1+\frac{\Delta t}{T_1}\right)$, centred at point $\left(0, \rho_1\left(1+\frac{\Delta t}{T_1}\right)\right)$. See Figure C.1 for an illustration of the cleared circle shifting and expanding in real-space and time. The solid $-\square-$ circle is the first dip footprint at time T_1 and represents the cleared circle at time T_1. As time

progresses to time T_2, the cleared circle expands north to the dashed $--\times--$ circle. The solid $-\times-$ circle is the second dip footprint at time T_2. The second dip is disjoint from the first if the solid $-\times-$ circle and dashed $--\times--$ circle do not overlap.

If the second dip is disjoint, the detection probability is $\frac{R^2}{\rho^2(T_1+\Delta t)}$. The best disjoint strategy corresponds to the smallest Δt that produces a disjoint dip, which occurs when the helicopter heads due south after the first dip. To compute this best disjoint time, which we denote Δt^D, we determine when the distance between the center of the cleared circle and the second dip location (the distance between the two $\times$ circle centers in Figure C.1) equals the sum of the two radii:

$$\rho_1\left(1+\frac{\Delta t^D}{T_1}\right)-(\rho_1-V\Delta t^D)=R\left(1+\frac{\Delta t^D}{T_1}\right)+R$$

$$\Rightarrow \Delta t^D=\frac{2R}{V+\frac{(\rho_1-R)}{T_1}} \qquad \text{(C.1)}$$

Any $\Delta t<\Delta t^D$ will produce overlap. We define $\text{overlap}(\Delta t)$ as the area of overlap when the next dip occurs at time $\Delta t<\Delta t^D$. To compute $\text{overlap}(\Delta t)$ requires calculating the area of intersection between the following two circles:

Cleared circle (dashed $--\times--$): center = $\left(0,\rho_1\left(1+\frac{\Delta t}{T_1}\right)\right)$, radius = $R\left(1+\frac{\Delta t}{T_1}\right)$

Footprint of second dip (solid $-\times-$): center = $\left(0,(\rho_1-v\Delta t)\right)$, radius = R

The formula for this area of intersection appears in standard geometric references (for examples, see equation (14) in Weisstein (2017)), and we provide it below for our context:

$$\text{overlap}(\Delta t) = R^2 \cos^{-1}\left(\frac{(d(\Delta t))^2 - R^2\left(\frac{\Delta t}{T_1}\right)^2}{2Rd(\Delta t)}\right)$$
$$+ R^2\left(1+\frac{\Delta t}{T_1}\right)^2 \cos^{-1}\left(\frac{(d(\Delta t))^2 + R^2\left(\frac{\Delta t}{T_1}\right)^2}{2R\left(1+\frac{\Delta t}{T_1}\right)d(\Delta t)}\right)$$
$$-\frac{1}{2}\sqrt{\left(-d(\Delta t)+R\left(2+\frac{\Delta t}{T_1}\right)\right)\left(d(\Delta t)-R\left(\frac{\Delta t}{T_1}\right)\right)\left(d(\Delta t)+R\left(\frac{\Delta t}{T_1}\right)\right)\left(d(\Delta t)+R\left(2+\frac{\Delta t}{T_1}\right)\right)},$$

where $d(\Delta t) = \left(\frac{\rho_1}{T_1} + V\right)\Delta t$ is the distance between the center of the cleared circle and the center of the second dip. To show that overlap can be optimal, we must find a $\Delta t < \Delta t^D$ such that

$$\frac{\pi R^2 - \text{overlap}(\Delta t)}{\pi\rho^2(T_1+\Delta t)} > \frac{\pi R^2}{\pi\rho^2(T_1+\Delta t^D)} \qquad \text{(C.2)}$$

In the next section we present two such examples.

Section C.2 Examples of Optimal Overlapping Dips

We set

- V = 11 kts
- U = 7 kts
- R = 3.5nm
- $T_1 = 1$ hour
- $\rho_1 = 3.5$ nm

The detection probability on the first dip is 0.25. Substituting into Equation (C.1) yields $\Delta t^D = 0.636$ hours. The largest detection probability from a disjoint dip is 0.093 (substitute into the right-hand side of (C.2)). Numerically optimizing the left-hand side of (C.2) yields $\Delta t^* = 0.838\Delta t^D = 0.533$ hours. This generates an overlap of

$\text{overlap}(\Delta t^*) = 3.25\,\text{nm}^2$ and a detection probability of 0.097. The optimal overlap dip occurs over 15% earlier than the disjoint dip and produces a detection probability 4% greater.

In the previous example, the differences between the disjoint dip and the optimal overlap dip are not trivial. However, the parameter values are not realistic as the helicopter will travel much faster than 11 kts. Below is a more realistic example where the disjoint dip is suboptimal

- V = 82 kts
- U = 13.8 kts
- R = 3nm
- $T_1 = 0.45$ hour
- $\rho_1 = 3.1$ nm

The optimal time of the next dip $\Delta t^* = 0.977\Delta t^D = 0.071$ is close to the time of the next disjoint dip and the optimal detection probability (0.1732) is only slightly better than the disjoint detection probability (0.1728).

The disjoint dip is not optimal when the helicopter arrives quickly to the datum. The difference between the disjoint dip and optimal dip is larger for slower helicopters. Thus, for realistic scenarios where the helicopter is much faster than the submarine, disjoint dips should perform near optimally.